nature portfolio

Peer Review File

5'-end binding pockets govern DICER cleavage fidelity

Corresponding Author: Dr Tuan Anh Nguyen

Any redactions in this file are there to maintain patient confidentiality, the confidentiality of unpublished data, or to remove third-party material.

This file contains all reviewer reports in order by version, followed by all author rebuttals in order by version.

Version 0:

Reviewer comments:

Referee #1

(Remarks to the Author)
The manuscript by Ngo et al. combines biochemical assays, cryo-electron microscopy, and mutational analysis to uncover a previously unrecognized mechanism by which DICER determines cleavage site selection during small RNA processing. Through systematic biochemical experiments, the authors demonstrated that the 5' terminal nucleotide—particularly 5'-G—plays a critical role in guiding DICER to cleave at specific sites, challenging the previous assumption that 5'-G impairs cleavage accuracy. Using cryo-EM structures of DICER bound to shRNAs with different 5' ends, the authors identified a novel 5'-G–favored binding pocket, distinct from the known 5'-U binding site. This structural discovery provides a mechanistic explanation for how the identity of the 5' nucleotide influences cleavage site selection and small RNA length. Moreover, the study reveals that the 5'-end counting rule and RNA structural motifs such as mWCU and YCR can work in coordination or in discoordination to guide DICER to cleave RNA at specific positions by inducing RNA conformational changes that realign the cleavage site with DICER's catalytic center. Together, this research is interesting and significant, as it introduces a dual-pocket model for 5' end recognition of Dicer that corresponds to cleavage specificity, offering new insights into how DICER selects cleavage sites and generates diverse small RNAs.

Comments:

1. The manuscript presents a previously unrecognized 5'-G binding pocket in the DICER protein through structural analysis and performs site-directed mutagenesis on key residues D991 and H992. The results shown in Fig. 3d,e demonstrate that these mutations not only reduce DICER's cleavage efficiency at the DC21 site for pre-miRNAs containing 5'-G, but also lead to an increase in cleavage activity at the DC22 site. Why do these mutations result in increased cleavage at the DC22 site for pre-miRNAs with 5'-G? Could the authors provide an explanation for this shift in cleavage preference?

2. The biochemical experiments in this study were conducted using pre-miRNAs and their variants, while the structural analysis was performed with shRNAs. Given that pre-miRNAs and shRNAs can differ in their RNA secondary structures, the authors should ideally determine the structure of DICER in complex with at least one endogenous pre-miRNA to confirm that the observed structural features are consistent with those of shRNAs, thereby strengthening the conclusions of the study.

3. The article proposes that the binding of 5'-G in its specific pocket induces a distinct upward shift in RNA positioning compared to 5'-U, aligning the DC21 cleavage site with DICER's catalytic center. However, in the DICER/26S-GU structure, this effect appears to be overridden by RNA motifs (such as mWCU and YCR), resulting in the alignment of DC22 with the catalytic center instead. To provide a clearer mechanistic explanation of how the 5'-nt influences cleavage site selection, the authors should present a structure of DICER/26S-GU in the absence of these RNA motifs. Such a structure would directly demonstrate whether 5'-G alone is sufficient to position DC21 at the catalytic center, thereby validating the proposed mechanism and strengthening the structural basis for 5'-end–mediated cleavage site determination.

4. The manuscript proposes that in the DICER/26S-GU structure, the R1855 in dsRBD is positioned closer to the 19-CC mismatch, and upon interaction, it may exert a stronger mechanical force on the RNA backbone, leading to a conformational change that shifts the alignment of the cleavage site from DC21 to DC22. Could the authors further demonstrate the functional importance of the interaction between DICER and the RNA motif in this process? For example, if the interaction between R1855 and the 19-CC mismatch is disrupted, does the structure show a restoration of DC21 cleavage site

alignment with the catalytic center?

5. The authors have demonstrated that the 5' terminal nucleotide plays a key role in determining DICER cleaves at the DC21 or DC22 site through in vitro biochemical and structural studies. At the same time, they also show that other factors, such as RNA motifs (e.g., mWCU and YCR), contribute to cleavage specificity. Given these findings, an important question arises: How functionally significant is the 5'-end–guided cleavage specificity in vivo? More specifically, what would be the biological consequences of disrupting the 5'-end counting rule in living organisms?

6. The authors suggest that when DICER binds long-stem shRNAs, the RNA duplex aligns closely with DICER's longitudinal axis, whereas shorter RNA substrates exhibit a more loosely aligned configuration. Whether this difference in dsRBD and PAZ domain positioning is directly driven by RNA–protein interactions is unclear. A more detailed RNA–protein interaction analysis may help elucidate the mechanism underlying DICER's adaptability to different substrates.

7. The authors refer to Ext. Data Fig. 8b in the text, but no corresponding figure is labeled or included in the figures.

8. The marker on the gel image is unclear and does not accurately indicate the positions of the RNA bands, such as Fig. 1b,e,i and Ext. Data Figs. 1g,j,m and 4a. The authors should clearly label the size (in nucleotides) of each marker band to facilitate accurate interpretation of the results.

Referee #2

(Remarks to the Author)
This manuscript reports structural and biochemical evidence for two distinct 5′-end binding pockets in human DICER: a guanosine-favored pocket that positions substrates for 21-nt cleavage (DC21) and the previously described uridine-favored pocket that positions for 22-nt cleavage (DC22). Contrary to earlier models (e.g., Kim et al., 2023) which suggested that 5′-G reduces cleavage accuracy, the authors show that 5′-G often enhances register precision toward DC21.

A key caveat is that the 5′-G structures presented here include strong DC22-favoring (mWCU/YCR) motifs, meaning the observed conformation reflects a motif-overridden state rather than the DC21-aligned state the model seeks to explain. As such, the structural basis for DC21 specificity is inferred from the geometry of the G-pocket, not directly visualized, and the effects of the 5′ nucleotide cannot be fully separated from those of the motifs.

Biochemical assays with pre-mir-517a variants and massively parallel dicing assays using pre-mir-324 confirm that 5′-G and 5′-A bias toward DC21, while 5′-U and 5′-C tend to favor DC22, though context and terminal base pairing can yield mixed outcomes. Cryo-EM structures of DICER bound to 5′-G and 5′-U shRNAs reveal alternative 5′-end binding modes and domain rearrangements in the PAZ and dsRBD domains that compact the RNA-binding cleft. Mutagenesis of G-pocket residues selectively impairs DC21 cleavage of 5′-G substrates.

When 5′-end preference conflicts with internal RNA motifs such as mWCU/YCR, motif-induced RNA distortions can override pocket-driven register selection. The authors propose a substrate-dependent “dual-pocket” & “motif override” mechanism for cleavage site choice, conserved across species. Overall, the biochemical work is strong, but key aspects of the structural analysis require clarification and much clearer visual explanation before publication.

Major points:

1. The structures presented for 5′-G substrates include strong DC22-favoring (mWCU/YCR) motifs, so the observed conformation reflects a motif-overridden state rather than the DC21-aligned state that the model seeks to explain. As such, the structural basis for DC21 specificity is inferred rather than directly visualized, and the effects of the 5′ nucleotide cannot be separated from those of the motifs. A 5′-G structure without these motifs would be needed to establish the DC21 mechanism more directly.

2. The identification of a distinct 5′-G–favored pocket is a central structural claim that needs stronger presentation. Clear experimental density and model fit for the key interactions (R821/D991/H992) should be shown. While the mutagenesis validation is a major strength, structural visualization is insufficient.

3. The proposed mechanism of substrate discrimination is difficult to follow from the current figures. Much of the analysis hinges on RMSD differences in dsRBD and PAZ domains relative to pre-let-7a-1GYM (PDB 7XW2) and apo DICER (PDB 7XW3), but the functional consequences of these domain motions for register selection are not clearly illustrated. The figure layouts focus on domain movements without showing a direct connection to RNA repositioning or cleavage-site alignment, making it hard for the reader to understand how these motions lead to DC21 vs. DC22 selection.

4. Fig. 1f shows that certain 3′ overhangs can influence cleavage accuracy for 5′-G and 5′-A substrates. This observation seems ignored in the manuscript and gives the impression that the proposed 5′-nt rules are over-simplified.

Other comments:

5. Expand Methods to include complete structural data collection and processing details, including detector type, exposure parameters, software versions, and processing workflow specifics.

6. In Fig. 1f, explicitly indicate the 5′ nucleotide for each block and group results visually to facilitate comparison across nucleotide classes.

7. Define all color schemes in Fig. 2h in the legend or within the panel itself.

8. Explain the significance of the green dashed circles in Fig. 3a,b and how they relate to the described binding pocket features.

9. Clarify the intended meaning of “intrinsic anisotropy” of DICER (line 144) and explain how it impacts the cryo-EM data or reconstruction quality.

Version 1:

Reviewer comments:

Referee #1

(Remarks to the Author)
The revised manuscript is significantly improved, and the authors have responded to my comments. The revised paper is now suitable for publication.

minor comment: In the main text, the legend for Figure 2C states: " Cleavage accuracy was calculated based on three independent assays (data shown in Extended Data Figure 2a), demonstrating precise cleavage at DC22." However, The current content of Extended Data Figure 2a seems unrelated to the DICER cleavage accuracy measurement. Please verify and correct the reference to the appropriate supplementary figure that contains the supporting data for Figure 2C.

Referee #2

(Remarks to the Author)
The authors have addressed my major concerns in their revised manuscript. Specifically, the addition of the DICER/pre-miR-517a_GU cryo-EM structure directly resolves the key structural gap identified in my initial review by visualizing a 5′-G substrate in a DC21-aligned register without confounding motif effects. Together with the accompanying biochemical and mutational data, the revised manuscript provides a well-supported mechanistic framework for 5′-end–dependent cleavage site selection. I have no further major concerns that would require additional experiments or delay editorial consideration.

Dear reviewers,
We sincerely thank the reviewers for your thoughtful and constructive feedback, as well as for recognizing the significance and interest of our work. Below, we address all of your concerns, incorporating additional experiments and revising the manuscript where necessary. Notably, beyond the two cryo-EM structures included in the initial submission, we now present three additional cryo-EM structures:

1. DICER bound to a different RNA substrate (pre-mir-517a),
2. Mutant DICER bound to the same substrate as before at the dicing state, and
3. DICER bound to pre-mir-517a at the pre-dicing state.

The changes addressing your questions are highlighted in blue. Additionally, we corrected many typos that we found but did not highlight them.
Below, we provide detailed responses to your questions.

Referee expertise:

Referee #1: sRNA function/biology

Referee #2: cryoEM, including of RNAi

Referees' comments:

Referee #1:

The manuscript by Ngo et al. combines biochemical assays, cryo-electron microscopy, and mutational analysis to uncover a previously unrecognized mechanism by which DICER determines cleavage site selection during small RNA processing. Through systematic biochemical experiments, the authors demonstrated that the 5' terminal nucleotide—particularly 5'-G—plays a critical role in guiding DICER to cleave at specific sites, challenging the previous assumption that 5'-G impairs cleavage accuracy. Using cryo-EM structures of DICER bound to shRNAs with different 5' ends, the authors identified a novel 5'-G–favored binding pocket, distinct from the known 5'-U binding site. This structural discovery provides a mechanistic explanation for how the identity of the 5' nucleotide influences cleavage site selection and small RNA length. Moreover, the study reveals that the 5'-end counting rule and RNA structural motifs such as mWCU and YCR can work in coordination or in discoordination to guide DICER to cleave RNA at specific positions by inducing RNA conformational changes that realign the cleavage site with DICER's catalytic center. Together, this research is interesting and significant, as it introduces a dual-pocket model for 5' end recognition of Dicer that corresponds to cleavage specificity, offering new insights into how DICER selects cleavage sites and generates diverse small RNAs.

Comments:

1. The manuscript presents a previously unrecognized 5'-G binding pocket in the DICER protein through structural analysis and performs site-directed mutagenesis on key residues D991 and H992. The results shown in Fig. 3d,e demonstrate that these mutations not only reduce DICER's cleavage efficiency at the DC21 site for pre-miRNAs containing 5'-G, but also lead to an increase in cleavage activity at the DC22 site. Why do these mutations result in increased cleavage at the DC22 site for pre-miRNAs with 5'-G? Could the authors provide an explanation for this shift in cleavage preference?

We propose that mutations in the 5′-G pocket have minimal impact on overall cleavage efficiency but markedly shift cleavage-site preference. In WT DICER, cleavage occurs at both DC21 and DC22; in the mutant, cleavage is redirected exclusively to DC22. Because total efficiency is comparable, the sum of WT products (DC21 + DC22) approximates the mutant output (DC22 only), explaining the apparent

increase in DC22 products for 5′-G pre-miRNAs in the mutant. We added: “These DICER mutations do not appear to affect overall cleavage efficiency but do influence site selection, suggesting a role in adjusting DICER positioning between the DC21 and DC22 registers.”
To probe mechanism, we solved a 3.29 Å cryo-EM structure of a 5′-G-pocket mutant (DICER-D991G-H992G) bound to 26S-GU. Unlike WT, where 5′-G docks into the 5′-G pocket, in DICER-D991G-H992G the 5′-G does not occupy this site and shifts toward the 5′-U pocket (Fig. 3f–h; Extended Data Fig. 6).

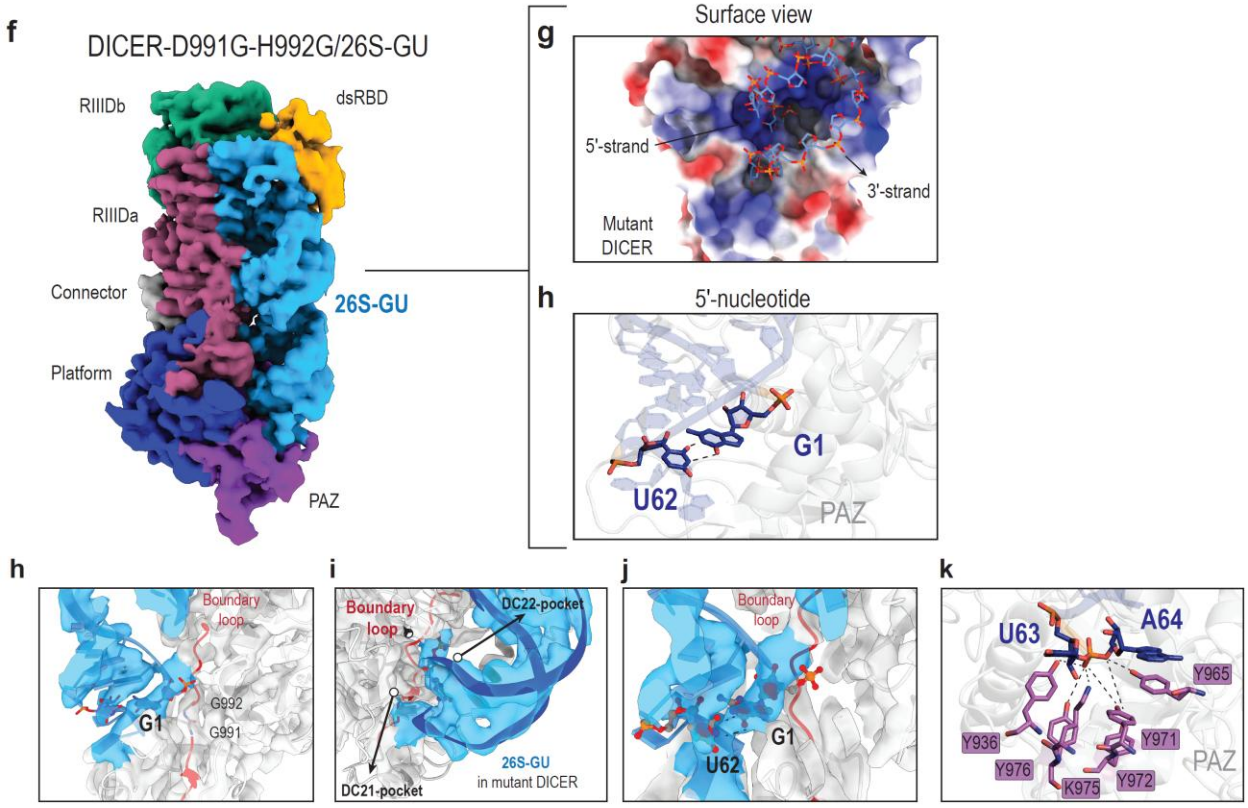

Together, these structures underscore the functional importance of the 5′-G pocket: in WT, specific 5′-G recognition stabilizes the DC21 register, whereas in the mutant, loss of this interaction permits reorientation toward the 5′-U pocket, redirecting cleavage to DC22.

2. The biochemical experiments in this study were conducted using pre-miRNAs and their variants, while the structural analysis was performed with shRNAs. Given that pre-miRNAs and shRNAs can differ in their RNA secondary structures, the authors should ideally determine the structure of DICER in complex with at least one endogenous pre-miRNA to confirm that the observed structural features are consistent with those of shRNAs, thereby strengthening the conclusions of the study.
We determined the structure of DICER bound to pre-miR-517a_GU, the substrate examined biochemically in our study, using an approach analogous to that for the DICER/26S complexes. Consistent with the 26S-GU structure, we obtained a 3.21 Å reconstruction and observed the pre-miRNA 5′-G engaged in the newly identified 5′-G pocket. These results further support the existence and functional relevance of the 5′-G binding pocket in DICER. See Fig. 4e–j and Extended Data Fig. 9.

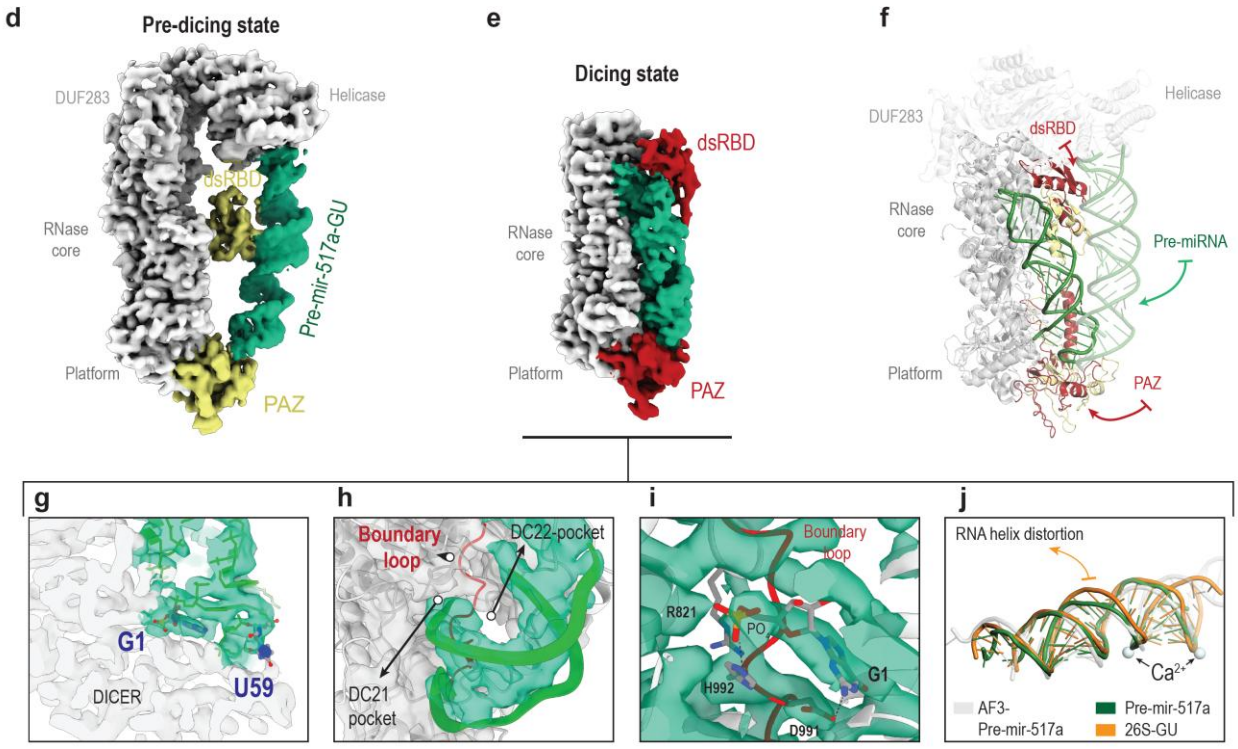
d
Pre-dicing state
DUF283
Helicase
dsRBD
RNase core
Pre-mir-517a-GU
Platform
PAZ
e
Dicing state
dsRBD
RNase core
Platform
PAZ
f
DUF283
Helicase
dsRBD
RNase core
Pre-miRNA
Platform
PAZ
g
G1
DICER
U59
h
Boundary loop
DC22-pocket
DC21 pocket
i
Boundary loop
R821
PO4
H992
G1
D991
j
RNA helix distortion
Ca2+
AF3-Pre-mir-517a
Pre-mir-517a
26S-GU

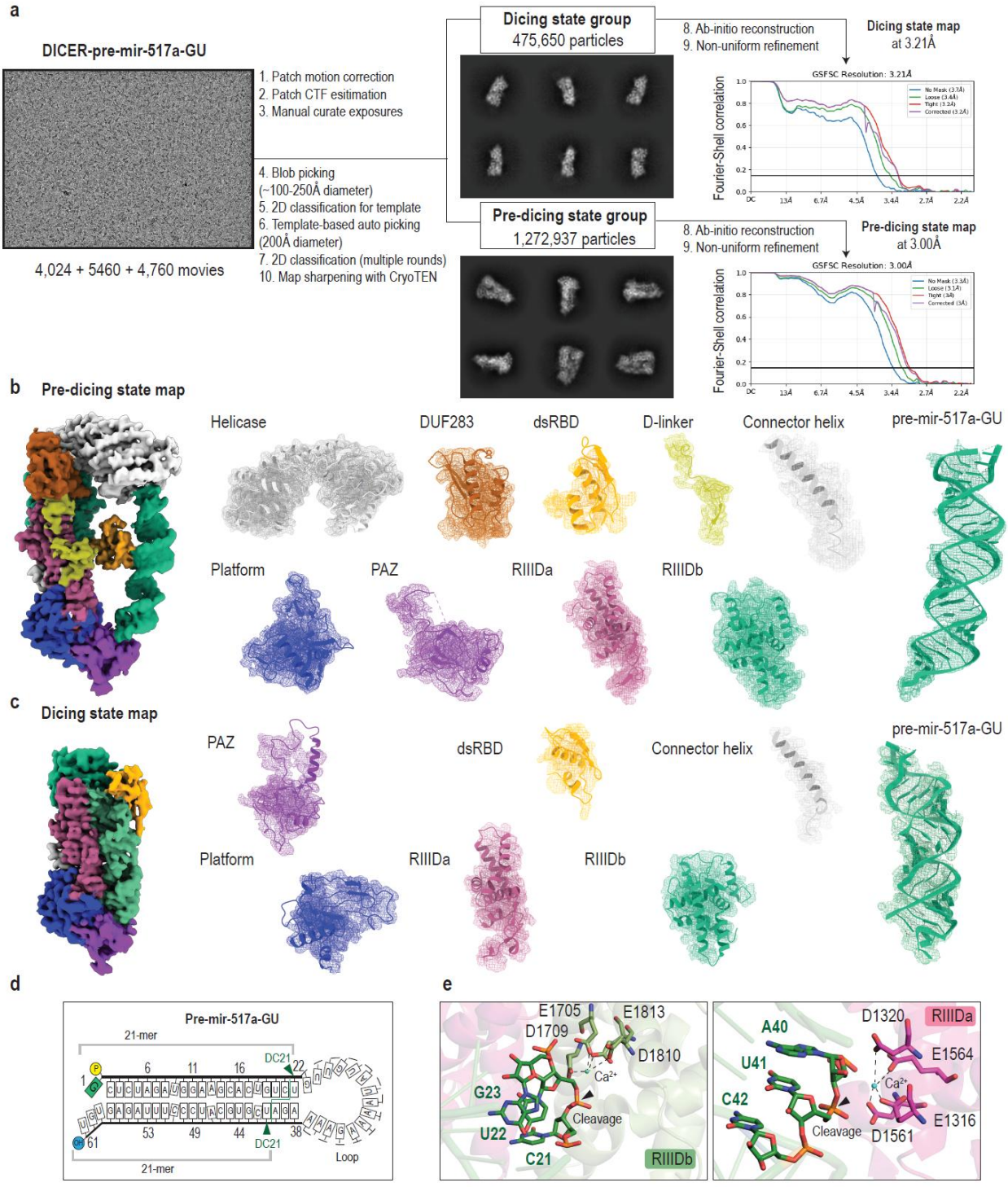
a
DICER-pre-mir-517a-GU
4,024 + 5460 + 4,760 movies
1. Patch motion correction
2. Patch CTF esitimation
3. Manual curate exposures
4. Blob picking
(~100-250Å diameter)
5. 2D classification for template
6. Template-based auto picking
(200Å diameter)
7. 2D classification (multiple rounds)
10. Map sharpening with CryoTEN
Dicing state group
475,650 particles
8. Ab-initio reconstruction
9. Non-uniform refinement
Dicing state map
at 3.21Å
GSFSC Resolution: 3.21Å
Fourier-Shell correlation
Pre-dicing state group
1,272,937 particles
8. Ab-initio reconstruction
9. Non-uniform refinement
Pre-dicing state map
at 3.00Å
GSFSC Resolution: 3.00Å
b
Pre-dicing state map
Helicase
DUF283
dsRBD
D-linker
Connector helix
pre-mir-517a-GU
Platform
PAZ
RIIIDa
RIIIDb
c
Dicing state map
PAZ
dsRBD
Connector helix
pre-mir-517a-GU
Platform
RIIIDa
RIIIDb
d
Pre-mir-517a-GU
21-mer
DC21
Loop
e
E1705
E1813
D1709
D1810
Ca2+
G23
Cleavage
U22
C21
RIIIDb
A40
D1320
RIIIDa
U41
E1564
C42
Ca2+
Cleavage
D1561
E1316

3. The article proposes that the binding of 5'-G in its specific pocket induces a distinct upward shift in RNA positioning compared to 5'-U, aligning the DC21 cleavage site with DICER's catalytic center. However, in the DICER/26S-GU structure, this effect appears to be overridden by RNA motifs (such as mWCU and YCR), resulting in the alignment of DC22 with the catalytic center instead. To provide a clearer mechanistic explanation of how the 5'-nt influences cleavage site selection, the authors should present a structure of DICER/26S-GU in the absence of these RNA motifs. Such a structure would directly demonstrate whether 5'-G alone is sufficient to position DC21 at the catalytic center, thereby validating the proposed mechanism and strengthening the structural basis for 5'-end–mediated cleavage site determination.

In 26S-GU, at least three elements, mWCU, YCR, and the long 26-bp stem, promote DC22 cleavage (refs. 1–3). Removing both motifs, or all three elements, increases DC21 cleavage for G-RNA (22S-GU). Comparing 22S-GU (5′-G) with 22S-UG (5′-U) further shows that 5′-G enhances DC21 cleavage; however, both constructs still yield mixed DC21/DC22 products. This dual-site outcome makes 26S-GU lacking motifs unsuitable for cryo-EM, which requires near-uniform site specificity to capture a single DICER–RNA conformation (Extended Data Fig. 11b).

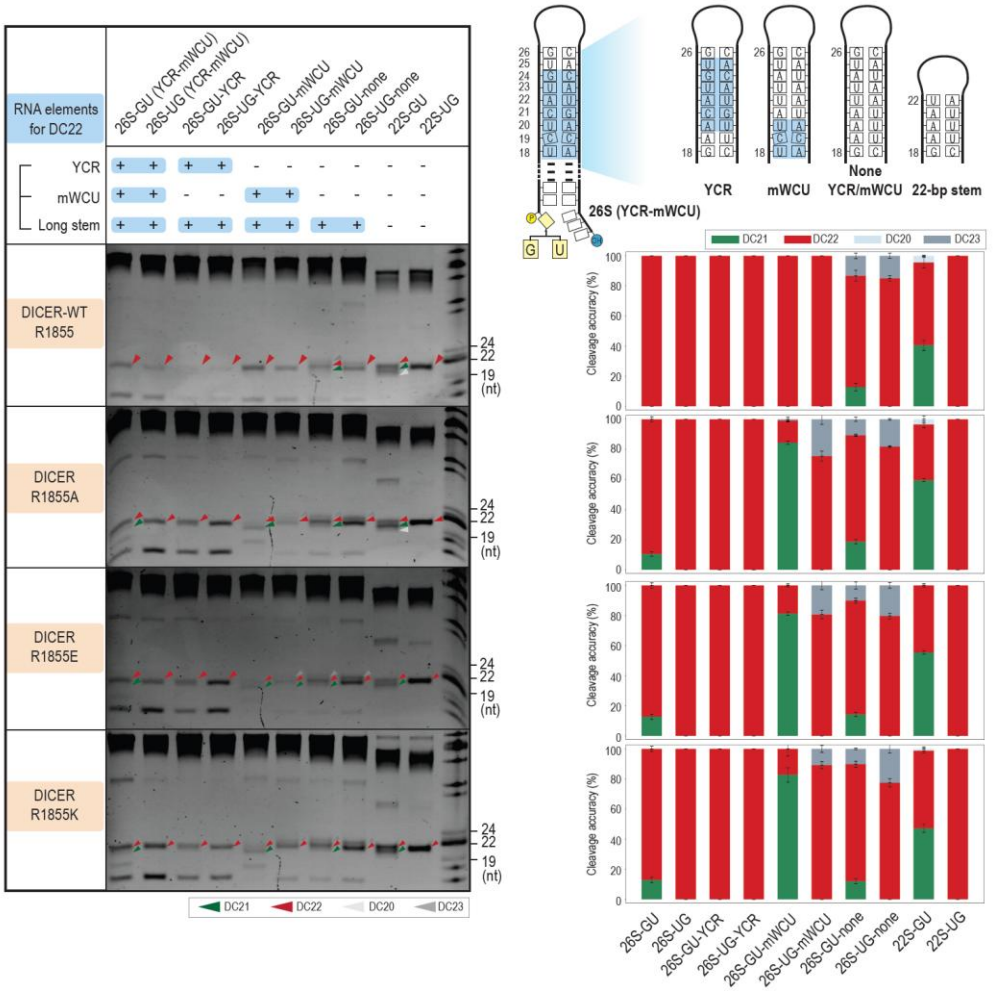

To overcome this, we determined the DICER/pre-miR-517a_GU structure. In this pre-miRNA, the 5′-G engages the newly identified 5′-G pocket, and DICER cleaves exclusively at DC21, providing a direct mechanistic explanation of how 5′-G dictates site selection.

References:

1. Nguyen, T. D., Trinh, T. A., Bao, S. & Nguyen, T. A. Secondary structure RNA elements control the cleavage activity of DICER. Nat. Commun. 13, 1–16 (2022).

2. Le, C. T., Nguyen, T. D. & Nguyen, T. A. Two-motif model illuminates DICER cleavage preferences. Nucleic Acids Res. 52, 1860–1877 (2024).
3. Le, T. N. Y., Le, C. T. & Nguyen, T. A. Determinants of selectivity in the dicing mechanism. Nat. Commun. 15, 1–16 (2024).

4. The manuscript proposes that in the DICER/26S-GU structure, the R1855 in dsRBD is positioned closer to the 19-CC mismatch, and upon interaction, it may exert a stronger mechanical force on the RNA backbone, leading to a conformational change that shifts the alignment of the cleavage site from DC21 to DC22. Could the authors further demonstrate the functional importance of the interaction between DICER and the RNA motif in this process? For example, if the interaction between R1855 and the 19-CC mismatch is disrupted, does the structure show a restoration of DC21 cleavage site alignment with the catalytic center?

Thank you for the suggestion. In 26S-GU, robust DC22 cleavage is promoted by three features: the long stem, the mWCU motif, and the YCR motif. Disrupting the DICER–mWCU contact by mutating R1855 to alanine (R1855A) caused only a modest decrease in DC22 with a slight increase in DC21. By contrast, when the 26S-GU mWCU construct lacked YCR, R1855A nearly abolished DC22 and shifted cleavage to DC21 with near-100% specificity, indicating that the R1855–mWCU interaction is critical for specifying DC22, particularly without YCR (Extended Data Fig. 11b).

Determining a cryo-EM structure of DICER-R1855A bound to 26S-GU mWCU (no YCR) would directly test whether DC21 is realigned with the catalytic center. However, DC21 cleavage by DICER-R1855A was not sufficiently homogeneous for high-resolution reconstruction, so we did not pursue this. Still, the predominant DC21 cleavage of 26S-GU mWCU (no YCR) is consistent with DC21 alignment in the absence of the R1855–mWCU interaction.

In the DICER/pre-miR-517a_GU structure—where the RNA has a 5′-G and lacks an mWCU motif at DC22—cleavage is exclusively at DC21. The 5′-G occupies the 5′-G pocket, and the RNA conformation closely matches the predicted structure without detectable distortion, supporting the idea that RNA geometry remains unperturbed when 5′-end binding and motif-driven cues are aligned (Fig. 4j).

5. The authors have demonstrated that the 5' terminal nucleotide plays a key role in determining DICER cleaves at the DC21 or DC22 site through in vitro biochemical and structural studies. At the same time, they also show that other factors, such as RNA motifs (e.g., mWCU and YCR), contribute to cleavage specificity. Given these findings, an important question arises: How functionally significant is the 5'-end–guided cleavage specificity in vivo? More specifically, what would be the biological consequences of disrupting the 5'-end counting rule in living organisms?

Thank you for the questions. Assessing in vivo consequences of disrupting the 5′-end counting rule would require engineering 5′-end mutations in specific pre-miRNAs and performing organismal studies, a substantial undertaking. As an interim step, we ectopically expressed pre-miR-517a bearing either a 5′-G or 5′-U in HCT116 DICER-KO cells together with DICER-WT or the DICER-D991G-H992G mutant. Consistent with our in vitro data, 5′-G pre-miR-517a produced more DC21 than 5′-U. Notably, in cells we observed a higher DC22:DC21 ratio than in DICER-only in vitro assays, suggesting TRBP involvement: in vitro, DICER/TRBP generated more DC21 than DC22, indicating TRBP modulates site selection. Moreover, both 5′-G and 5′-U pre-miR-517a yielded similar DC21/DC22 levels with DICER-D991G-H992G, and these were lower than 5′-G processed by DICER-WT, supporting the importance of the 5′-G region for recognition by the DH residues (Extended Data Fig. 5f–h).

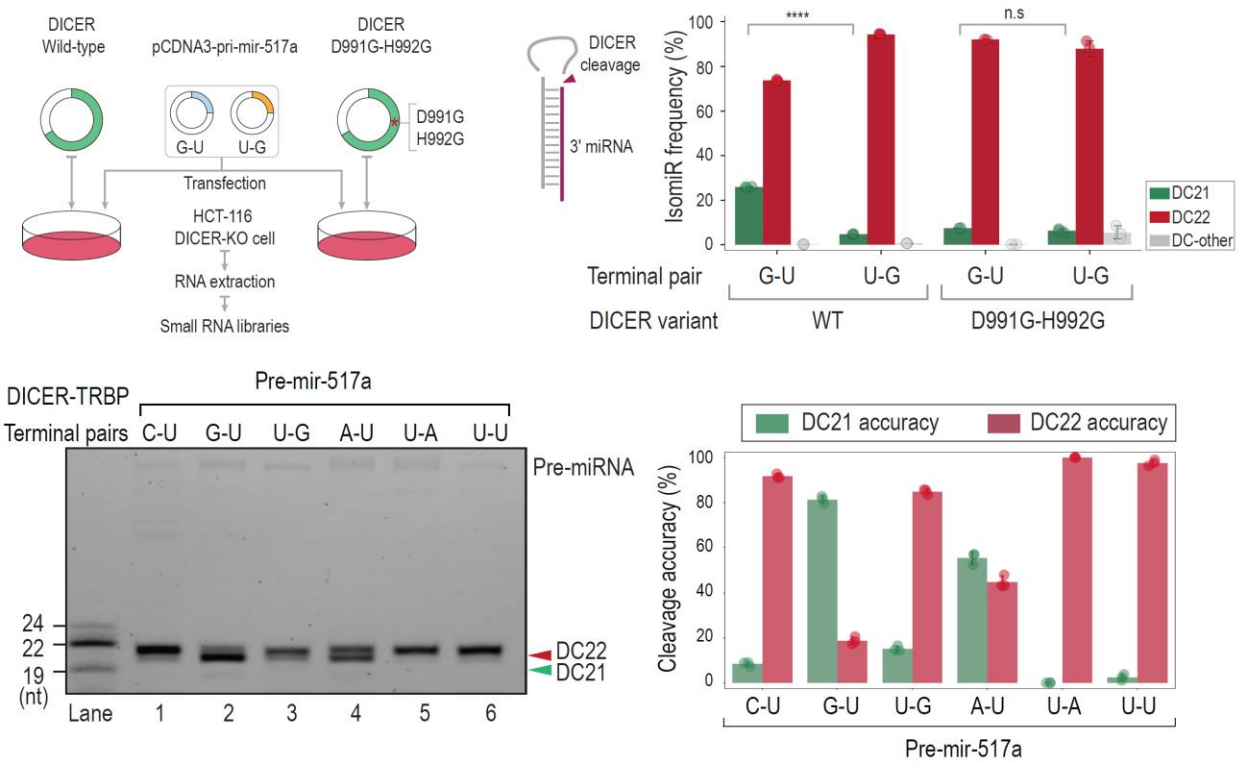

We also analyzed miRNA datasets across multiple animal species. In all species examined, 5′-G pre-miRNAs produced a higher fraction of DC21 products, whereas 5′-U pre-miRNAs produced more DC22 products, consistent with our in vitro observations (Extended Data Fig. 7g,h).

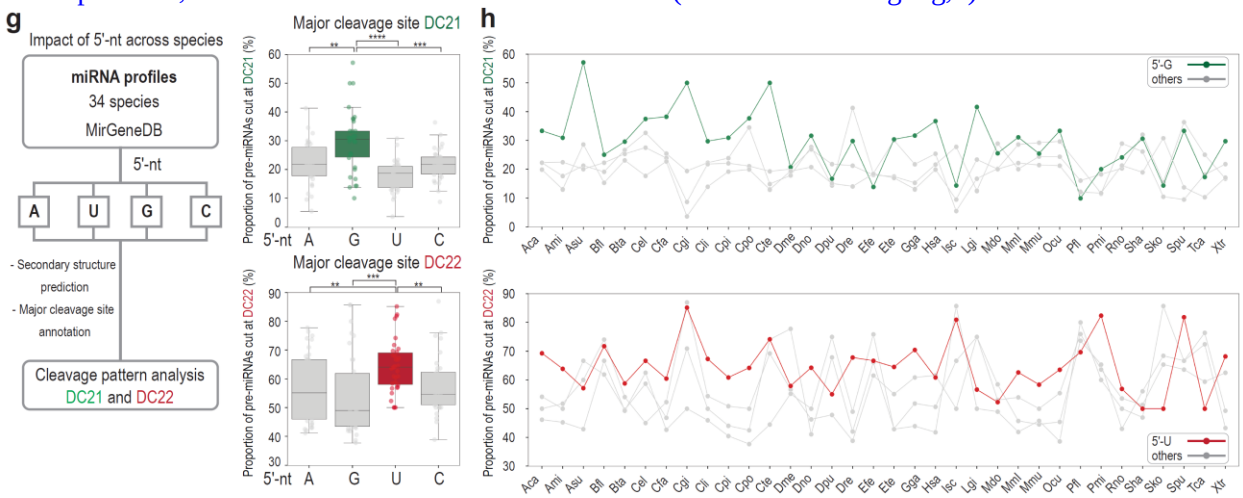

6. The authors suggest that when DICER binds long-stem shRNAs, the RNA duplex aligns closely with DICER's longitudinal axis, whereas shorter RNA substrates exhibit a more loosely aligned configuration. Whether this difference in dsRBD and PAZ domain positioning is directly driven by RNA–protein interactions is unclear. A more detailed RNA–protein interaction analysis may help elucidate the mechanism underlying DICER's adaptability to different substrates.

Thank you for raising this point. We compared the interactions of the dsRBD and PAZ domains with pre-let-7a-1 and the three RNAs from our solved structures in this study. Our analysis revealed that the

dsRBD interacts with these RNAs in a largely similar manner. However, in our solved structures, where the RNA duplex aligns closely with DICER's longitudinal axis, we observed a distinct curvature of the 3-nt overhang at the termini of the RNAs.
Upon closer inspection of the protein and RNA structures, we identified that in our structures, certain residues within the PAZ domain may interact with the bases of these nucleotides, rather than exclusively with the phosphate groups, as observed in the pre-let-7a-1 structure. This suggests that PAZ–RNA interactions may play an additional role in stabilizing the RNA duplex alignment along DICER's longitudinal axis for longer RNA substrates. These results are presented in Extended Data Fig. 10b.

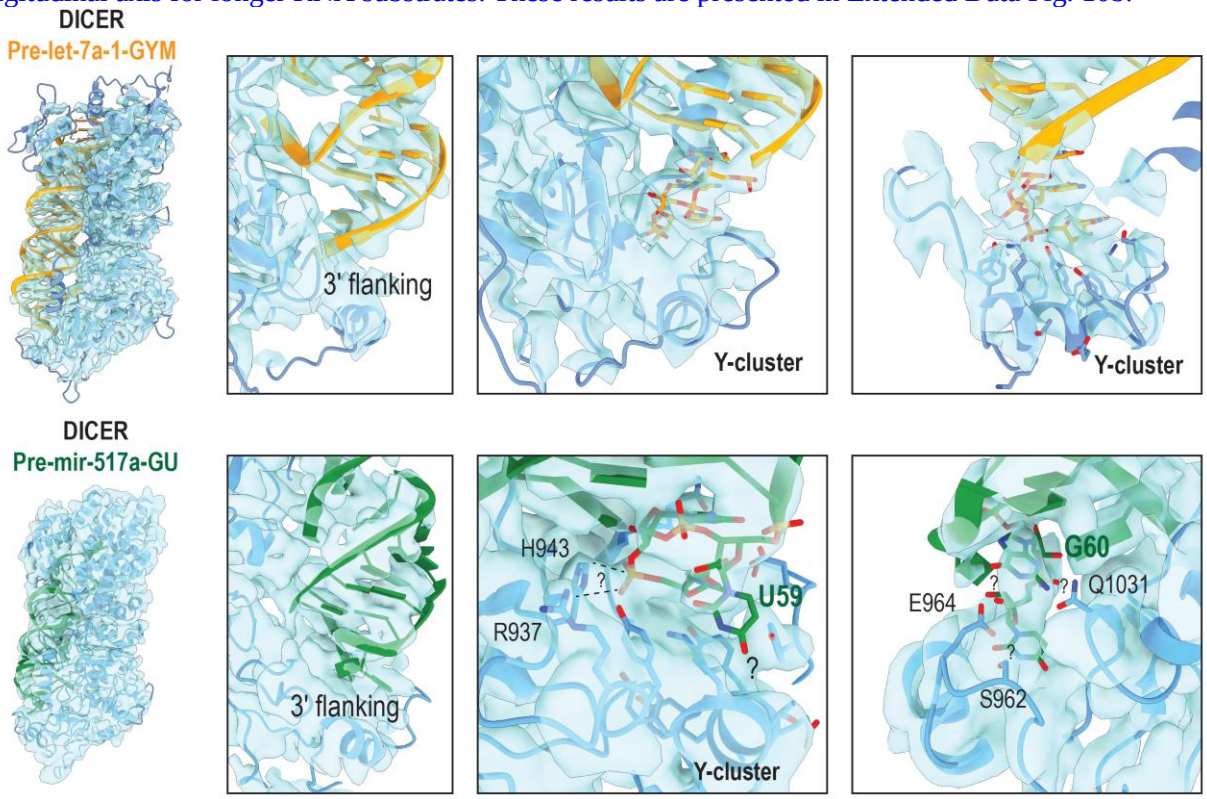

We added the text below in the revision:
"In addition, in pre-let-7a-1, PAZ appears to contact the terminal nucleotide, and the last three nucleotides look strained. By contrast, in pre-miR-517a and 26S RNAs, the 3′-terminal nucleotides are curved; in pre-miR-517a, where density is better resolved, the second and third overhang nucleotides may contact specific residues (Extended Data Fig. 10b). These patterns suggest that DICER adapts to different RNA substrates."

7. The authors refer to Ext. Data Fig. 8b in the text, but no corresponding figure is labeled or included in the figures.
We apologize for the error. The panel labeled "Extended Data Figure 8e" should have been "Extended Data Figure 8b." We have corrected this, and it is now presented as "Extended Data Figure 11a."

8. The marker on the gel image is unclear and does not accurately indicate the positions of the RNA bands, such as Fig. 1b,e,i and Ext. Data Figs. 1g,j,m and 4a. The authors should clearly label the size (in nucleotides) of each marker band to facilitate accurate interpretation of the results.

Thank you for the suggestion. We have now clearly labeled the RNA markers on all gels.

Referee #2:

This manuscript reports structural and biochemical evidence for two distinct 5′-end binding pockets in human DICER: a guanosine-favored pocket that positions substrates for 21-nt cleavage (DC21) and the previously described uridine-favored pocket that positions for 22-nt cleavage (DC22). Contrary to earlier models (e.g., Kim et al., 2023) which suggested that 5′-G reduces cleavage accuracy, the authors show that 5′-G often enhances register precision toward DC21.

A key caveat is that the 5′-G structures presented here include strong DC22-favoring (mWCU/YCR) motifs, meaning the observed conformation reflects a motif-overridden state rather than the DC21-aligned state the model seeks to explain. As such, the structural basis for DC21 specificity is inferred from the geometry of the G-pocket, not directly visualized, and the effects of the 5′ nucleotide cannot be fully separated from those of the motifs.

Biochemical assays with pre-mir-517a variants and massively parallel dicing assays using pre-mir-324 confirm that 5′-G and 5′-A bias toward DC21, while 5′-U and 5′-C tend to favor DC22, though context and terminal base pairing can yield mixed outcomes. Cryo-EM structures of DICER bound to 5′-G and 5′-U shRNAs reveal alternative 5′-end binding modes and domain rearrangements in the PAZ and dsRBD domains that compact the RNA-binding cleft. Mutagenesis of G-pocket residues selectively impairs DC21 cleavage of 5′-G substrates.

When 5′-end preference conflicts with internal RNA motifs such as mWCU/YCR, motif-induced RNA distortions can override pocket-driven register selection. The authors propose a substrate-dependent “dual-pocket” & “motif override” mechanism for cleavage site choice, conserved across species. Overall, the biochemical work is strong, but key aspects of the structural analysis require clarification and much clearer visual explanation before publication.

Major points:

1. The structures presented for 5′-G substrates include strong DC22-favoring (mWCU/YCR) motifs, so the observed conformation reflects a motif-overridden state rather than the DC21-aligned state that the model seeks to explain. As such, the structural basis for DC21 specificity is inferred rather than directly visualized, and the effects of the 5′ nucleotide cannot be separated from those of the motifs. A 5′-G structure without these motifs would be needed to establish the DC21 mechanism more directly.

Thank you for your question. It is similar to point 3 from Reviewer 1. For consistency, we have copied our response from above here to address your comment.
In 26S-GU, at least three elements, mWCU, YCR, and the long 26-bp stem, promote DC22 cleavage (refs. 1–3). Removing both motifs, or all three elements, increases DC21 cleavage for G-RNA (22S-GU). Comparing 22S-GU (5′-G) with 22S-UG (5′-U) further shows that 5′-G enhances DC21 cleavage; however, both constructs still yield mixed DC21/DC22 products. This dual-site outcome makes 26S-GU lacking motifs unsuitable for cryo-EM, which requires near-uniform site specificity to capture a single DICER–RNA conformation (Extended Data Fig. 11b).

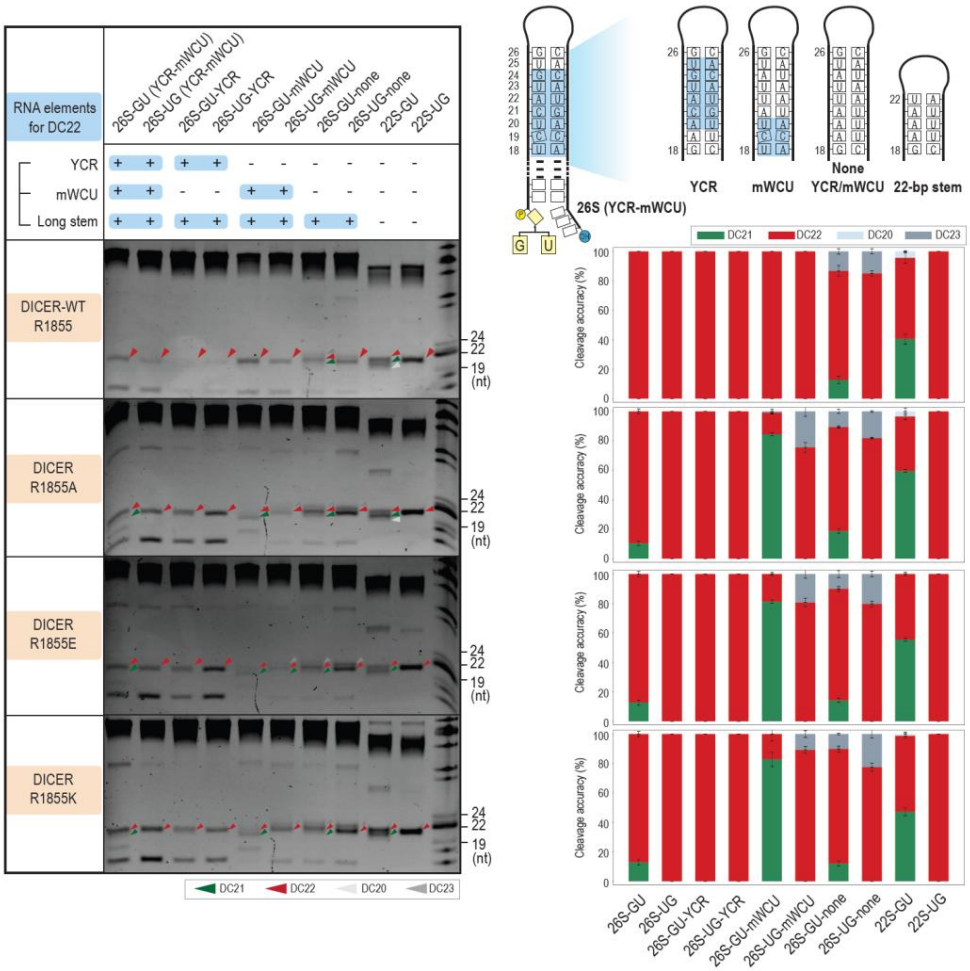

To overcome this, we determined the DICER/pre-miR-517a_GU structure. In this pre-miRNA, the 5′-G engages the newly identified 5′-G pocket, and DICER cleaves exclusively at DC21, providing a direct mechanistic explanation of how 5′-G dictates site selection.

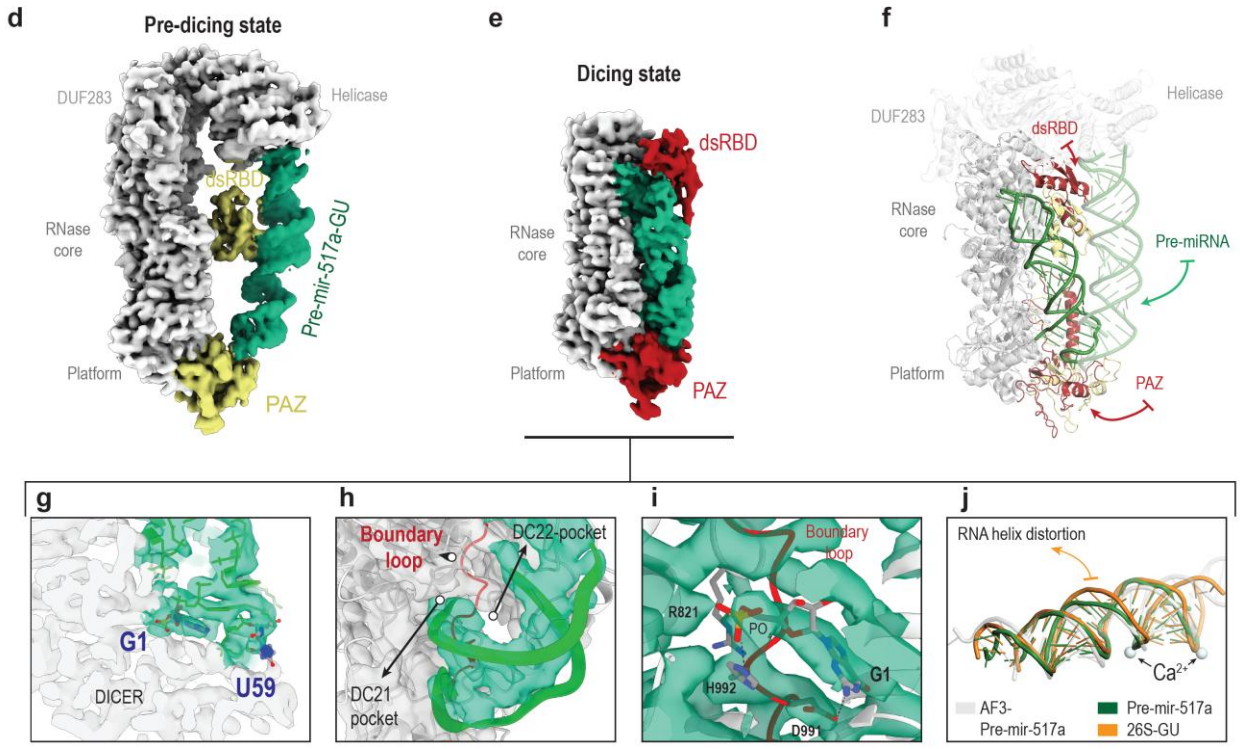

References:

1.
2. Nguyen, T. D., Trinh, T. A., Bao, S. & Nguyen, T. A. Secondary structure RNA elements control the cleavage activity of DICER. Nat. Commun. 13, 1–16 (2022).
3. Le, C. T., Nguyen, T. D. & Nguyen, T. A. Two-motif model illuminates DICER cleavage preferences. Nucleic Acids Res. 52, 1860–1877 (2024).
4. Le, T. N. Y., Le, C. T. & Nguyen, T. A. Determinants of selectivity in the dicing mechanism. Nat. Commun. 15, 1–16 (2024).

2. The identification of a distinct 5′-G–favored pocket is a central structural claim that needs stronger presentation. Clear experimental density and model fit for the key interactions (R821/D991/H992) should be shown. While the mutagenesis validation is a major strength, structural visualization is insufficient.
Thank you for the suggestion. In this revision, we present structures of both the DICER/pre-miR-517a_GU and DICER/26S-GU complexes (from the initial submission). For both, we now provide the experimental density and model fits for the key interactions involving D991 and H992. R821 is not well resolved; accordingly, we revise the key 5′-G/DICER interaction to highlight D991 and H992. The new figures are shown in Extended Data Fig. 5a and Fig. 4i.

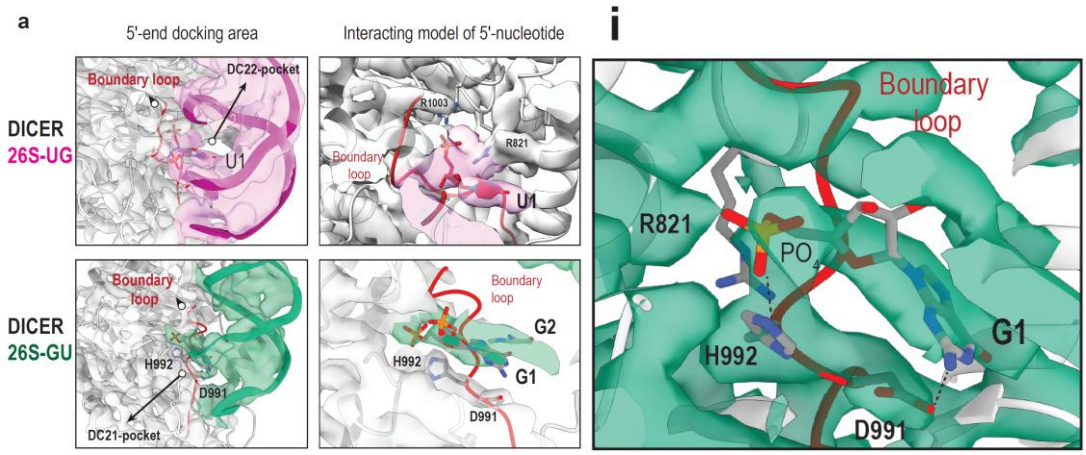

In addition, we solved the structure of the DICER-D991G-H992G mutant bound to 26S-GU, which shows loss of interaction density between the 5′-G and the 5′-G binding pocket. These data are presented in Extended Data Fig. 6h–j.

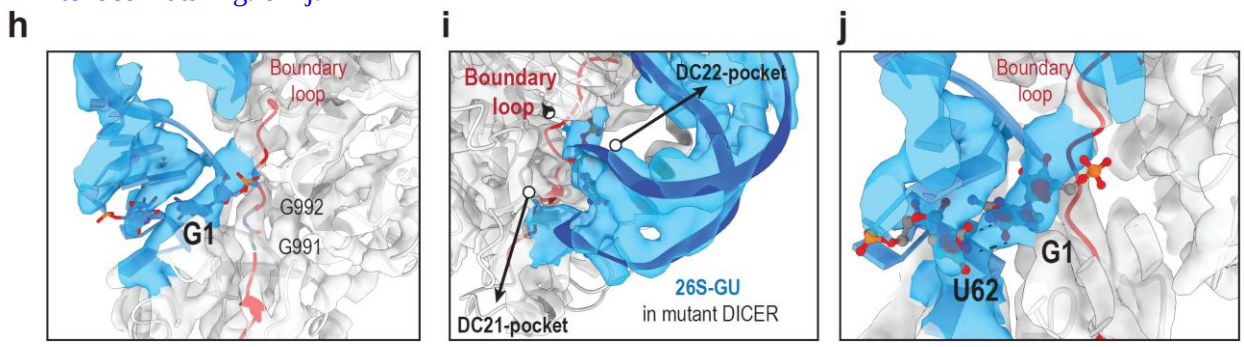

3. The proposed mechanism of substrate discrimination is difficult to follow from the current figures. Much of the analysis hinges on RMSD differences in dsRBD and PAZ domains relative to pre-let-7a-1GYM (PDB 7XW2) and apo DICER (PDB 7XW3), but the functional consequences of these domain motions for register selection are not clearly illustrated. The figure layouts focus on domain movements without showing a direct connection to RNA repositioning or cleavage-site alignment, making it hard for the reader to understand how these motions lead to DC21 vs. DC22 selection.

Thank you for your feedback, and we apologize for the lack of clarity in this section. The movements of the PAZ and dsRBD domains serve to align the RNA duplex with DICER's catalytic center, ensuring that both strands are correctly positioned over the two catalytic sites to enable double-strand cleavage. However, this alignment step itself does not determine whether DICER cleaves at DC21 or DC22. We have revised the text as follows:

"We propose that the dsRBD and PAZ domains function like "chopsticks," gripping and aligning RNA substrates to ensure precise double cleavages on both the 5'- and 3'-strands (Fig. 2j). In our structures with shRNAs, the RNA duplex remains tightly aligned without expansion (Extended Data Fig. 4e). However, in pre-let-7a-1-GYM from 7XW2, the dsRBD and PAZ domains are positioned farther from the RNA duplex. This conformation requires a widening of the RNA helix, as previously reported[13], to ensure proper alignment of both cleavage sites on the 5'- and 3'-strands with the catalytic center, facilitating accurate double cleavage (Extended Data Fig. 4f)."

In addition, while attempting to capture the dicing state of DICER with pre-miR-517a, we also resolved a pre-dicing state of the same complex at 3.0 Å resolution. A pre-dicing state had previously been observed for DICER–TRBP bound to a pre-miRNA at 4.7 Å resolution (PDB: 5ZAL) (1); however, the dicing state was not captured in that study. Another study visualized the dicing state with pre-let-7a-1 (2) (PDB: 7XW2). This study represents the first time both the pre-dicing and dicing states have been resolved for the same RNA, allowing us to track the movements of the PAZ and dsRBD domains across these two states. We present our new results in Fig. 4d-f and Extended Data Fig. 9.

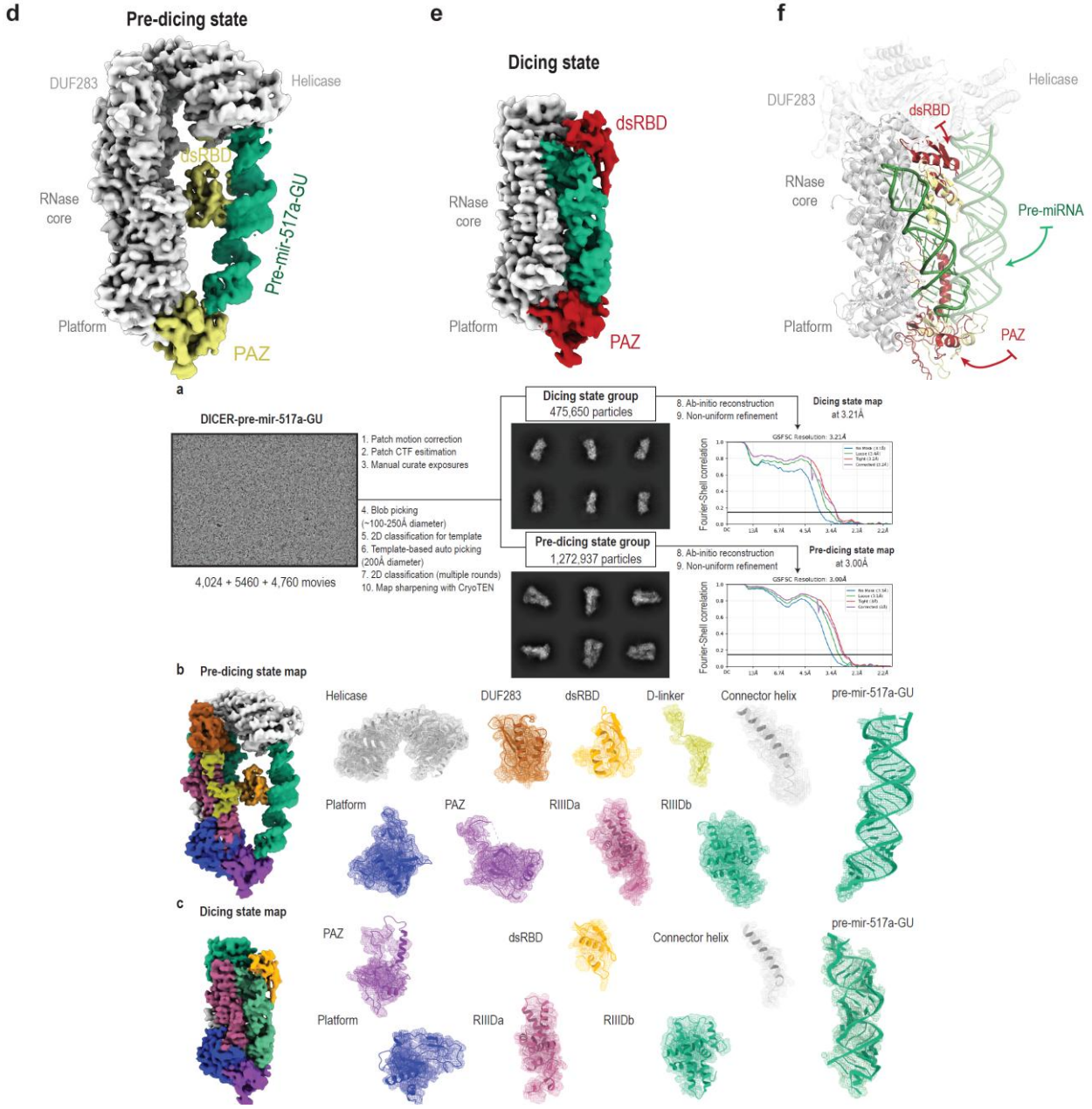

References:

1. Liu, Z. et al. Cryo-EM Structure of Human Dicer and Its Complexes with a Pre-miRNA Substrate. *Cell* **173**, 1191–1203.e12 (2018).

2. Lee, Y. Y., Lee, H., Kim, H., Kim, V. N. & Roh, S. H. Structure of the human DICER–pre-miRNA complex in a dicing state. *Nature* **615**, 331–338 (2023).

4. Fig. 1f shows that certain 3′ overhangs can influence cleavage accuracy for 5′-G and 5′-A substrates. This observation seems ignored in the manuscript and gives the impression that the proposed 5′-nt rules are over-simplified.

Thank you for your thoughtful question. Our additional analysis suggests that the nucleotide at the third position from the 3′ end can indeed influence DICER cleavage when the 5′ nucleotide is G or A, aligning with your observation. To fully dissect this effect, a dedicated panel of RNAs with systematically varied terminal pairs, particularly those with 5′-G and 5′-A, will be required. Generating and testing such a panel will take additional time. Therefore, in this revision, we prefer to discuss the observation rather than include preliminary data. However, we are happy to provide the data if requested during review.
We have added the below sentences to the manuscript:

"This study shows that the 5′-end nucleotide is a primary determinant of DICER cleavage at DC21 versus DC22, whereas the terminal 3′ nucleotide generally does not affect site choice. However, in 5′-A and 5′-G pre-miRNAs, cleavage sites are more variable than in other groups (Fig. 1f,g), suggesting that the 3-nt segment at the 3′ end may exert a stronger influence in this subset. Additional biochemical and structural analyses will be needed to clarify this effect."

5. Expand Methods to include complete structural data collection and processing details, including detector type, exposure parameters, software versions, and processing workflow specifics.
We have updated the *Cryo-EM Specimen Preparation* and *Cryo-EM Data Processing and 3D Refinement* sections to include the requested details, such as detector type, exposure parameters, software versions, and specifics of the processing workflow, as suggested by the reviewer.
The revised methods as below:
"**Cryo-EM specimen preparation**
The assembled samples for both DICER/26S-GU and DICER/26S-UG complexes were prepared using the same protocol. An aliquot of approximately 4 µL of sample was applied to glow-discharged

Quantifoil® R 2/2, 300 Mesh, Cu grids. After application, the sample was blotted at 100% humidity and 4°C, followed by vitrification in liquid ethane using a Vitrobot Mark IV (Thermo Fisher Scientific; blot force 0, wait time 30s, blotting time 4s with blotting paper No.2) at the Biological Cryo-EM Center at HKUST. Cryo-EM sample preparation for DICER/pre-miR-517a_GU and DICER-D991G/H992G/26S-GU followed the DICER/26S-GU protocol, except we used Quantifoil R 1.2/1.3, 400-mesh Au grids. Grids were screened on a Thermo Scientific Glacios at 200 keV, and those with evenly distributed particles and suitable ice thickness were selected for data collection.

Data collection was carried out using a Thermo Scientific 300 kV Titan Krios G3i cryo-TEM microscope located at the Biological Cryo-EM Center (HKUST). Microscope settings: Gatan K3 direct electron detector in counting mode; nominal magnification 81,000× (physical pixel size 1.051 Å). Exposure: total dose 50 e−/Å², fractionated into 40 frames (3.1 s total), dose rate ~17.7 e−/pix/s, ~1.25 e−/Å² per frame. Defocus: −1.0 to −2.4 µm.

For the DICER/26S-GU complex, 23,300 movies were collected from five datasets. The DICER/26S-UG complex included 11,241 movies from three datasets, DICER-D991G-H992G/26S-GU had 16,972 movies from two datasets, and DICER/pre-mir-517a_GU had 14,244 movies from three datasets. Detailed data collection parameters for these complexes are provided in Extended Data Table 1.

Cryo-EM data processing and 3D refinement

All image processing was performed in cryoSPARC v4.6.2 (Structura Biotechnology). Movies were corrected using Patch Motion Correction with default settings and binned to the physical pixel size, and CTF parameters were estimated per micrograph using Patch CTF Estimation (with default setting, fit range ~4–25 Å). Micrographs with poor CTF fits, thick ice, or contamination were excluded based on manual inspection.

Particles were initially identified by blob picking (radii 100–250 Å) and extracted in boxes of 256 pixels, followed by multiple rounds of 2D classification to remove junk and retain views characteristic of the DICER/RNA dicing state. High-quality 2D classes were used as templates for template-based auto-picking (particle diameter 200 Å), after which additional 2D cleaning was performed. Cleaned particle sets of ~ 181,000 particles were seeded for ab initio reconstruction (C1-symmetry) to obtain initial volumes. The appropriate initial volume resembled DICER and RNA complexes were selected and further refined with non-uniform refinement to obtain refined map.

The final DICER/26S-UG map (641,317 particles) reached 3.34 Å resolution by GS-FSC, and the DICER/26S-GU map (1,755,133 particles) reached 3.37 Å. The map of DICER-D991G-H992G/26S-GU (787,381 particles) reached 3.29 Å resolution by GS-FSC. The maps of DICER/pre-mir-517a_GU in pre-dicing (1,272,937 particles) and dicing state (475,650) reached 3.00 Å and 3.21 Å resolution by GS-FSC, respectively. Maps were sharpened with CryoTEN (default settings) to obtain final map for model building.

Model building

The current model of the DICER protein in the dicing state with pre-let-7a-1^{GYM} (PDB: 7XW2) was used as the initial protein model for both the DICER/26S-GU, DICER/26S-UG, DICER/pre-mir-517a_GU in dicing state maps. The initial RNA models for 26S-UG, 26S-GU, pre-mir-517a_GU were generated using AlphaFold3 for 3D RNA structure prediction[51]. The refined DICER/26S-GU model served as the starting model for DICER-D991G/H992G/26S-GU; D991G and H992G mutations were introduced in ChimeraX v1.7. For the DICER/pre-miR-517a_GU pre-dicing state, the apo structure (PDB 7XW3) was used as the initial model. These initial models were aligned with the cryo-EM density maps using the *Fit-in-Map* tool in ChimeraX version 1.7, followed by manual refinement in Coot (WinCoot version 0.9.8.96)[52,53]. The manually fitted models were further refined using *phenix.real_space_refine* in Phenix (version 1.20.1)[54]. Model validation was conducted with *phenix.validation_cryoem*[54].

All figures presented in the manuscript were created using ChimeraX version 1.7[52] and PyMOL (Schrödinger)[55].”

6. In Fig. 1f, explicitly indicate the 5′ nucleotide for each block and group results visually to facilitate comparison across nucleotide classes.

We have added the 5′ nucleotide labels for each block and grouped the results by nucleotide class to facilitate direct comparison. Thank you for the helpful suggestion.

7. Define all color schemes in Fig. 2h in the legend or within the panel itself.
We have defined the color scheme for this figure in the figure legend and revised the legend as shown below. Thank you.

"(**h**) Curvature of the 3′-overhang induced by PAZ domain movement. The PAZ domain adopts an 'inner' conformation (PAZ-in) in the DICER/26S-UG and DICER/26S-GU complexes, compared to the 'outer' conformation (PAZ-out) observed in DICER/pre-let-7a-1GYM (7XW2). The PAZ-in conformation induces bending of the 3′-overhang, optimizing RNA alignment for cleavage. The platform domain is shown in gray, the PAZ domain in purple, and the 3′ nucleotide at the RNA 3′ end is highlighted in yellow. RNA colors are light blue for pre-let-7a-1GYM, green for 26S-GU, and red for 26S-UG."

8. Explain the significance of the green dashed circles in Fig. 3a,b and how they relate to the described binding pocket features.
We apologize for not indicating the meaning of the green dashed line; it marks the 5′-G binding pocket in this figure. In response to your question, we now present the figure with an electrostatic surface representation to better visualize the two pockets. The updated figures are shown below.

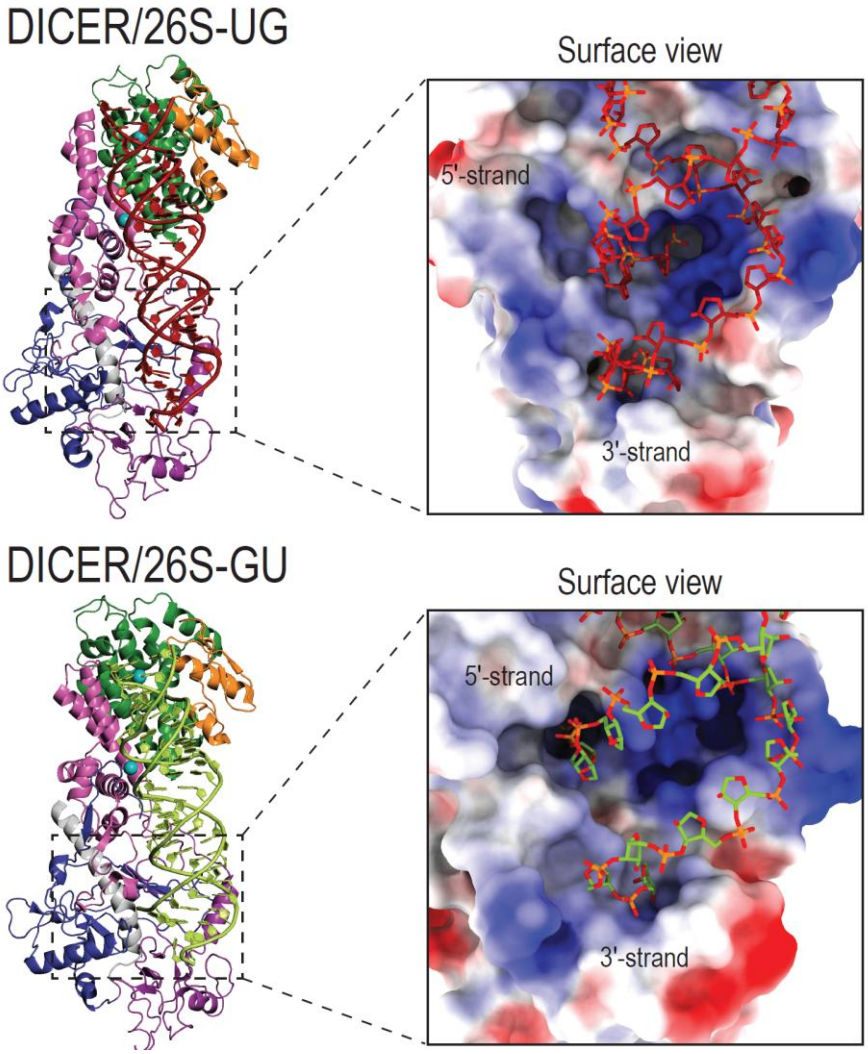

9. Clarify the intended meaning of "intrinsic anisotropy" of DICER (line 144) and explain how it impacts the cryo-EM data or reconstruction quality.

We thank you for the suggestion. We added the underlined clarification.

"A bias in particle orientation distribution was observed, consistent with the earlier structural study[13], which may result from the intrinsic anisotropy of the DICER protein, i.e., its asymmetric shape and mass distribution that promote preferred orientations on the grid (Extended Data Fig. 2f, Extended Data Fig. 3f). This preferential orientation can reduce directional resolution and lead to anisotropic reconstructions, potentially limiting map quality in certain directions."

Dear reviewers,

We sincerely thank the reviewers for their thoughtful and constructive feedback, as well as their support for the publication of our manuscript. Below, we address a final comment from Reviewer 1.

Referee #1 (Remarks to the Author):

The revised manuscript is significantly improved, and the authors have responded to my comments. The revised paper is now suitable for publication.

minor comment: In the main text, the legend for Figure 2C states: " Cleavage accuracy was calculated based on three independent assays (data shown in Extended Data Figure 2a), demonstrating precise cleavage at DC22." However, The current content of Extended Data Figure 2a seems unrelated to the DICER cleavage accuracy measurement. Please verify and correct the reference to the appropriate supplementary figure that contains the supporting data for Figure 2C.

Reponses: We thank Reviewer 1 for identifying this issue. We apologize for mistakenly citing the incorrect figure in this instance. The correct reference should be Extended Data Figure 3a instead of Extended Data Figure 2a. This error has been corrected in the revised manuscript.

Referee #2 (Remarks to the Author):

The authors have addressed my major concerns in their revised manuscript. Specifically, the addition of the DICER/pre-miR-517a_GU cryo-EM structure directly resolves the key structural gap identified in my initial review by visualizing a 5′-G substrate in a DC21-aligned register without confounding motif effects. Together with the accompanying biochemical and mutational data, the revised manuscript provides a well-supported mechanistic framework for 5′-end–dependent cleavage site selection. I have no further major concerns that would require additional experiments or delay editorial consideration.

Reponses: We sincerely thank Reviewer 2 for their support and positive feedback on our revised manuscript.